Electrochemical Investigation of Some Ruthenium-Carborane Complexes at a Glassy Carbon Electrode

Mohamed M. Ghoneim and **Ibrahim S. El-Hallag**[*]

Chemistry Department, Faculty of Science, Tanta University, Tanta, Egypt

Summary. Ruthenium complexes of some carboranes were examined using cyclic voltammetry, chronoamperometry, chronopotentiometry, and digital simulation techniques derived from convolution-deconvolution voltammetry. The complexes under consideration are of the type X-RuC$_2$B$_8$H$_{10}$ (X = hexamethylbenzene, *para*-cymene); all relevant electrochemical and chemical parameters were deduced and a mechanism is proposed.

Keywords. Ruthenium-carborane complexes; Hexamethylbenzene; *para*-Cymene; Cyclic voltammetry; Digital simulation.

Elektrochemische Untersuchung einiger Ruthenium-Carboran-Komplexe an einer Glaskohlenstoffelektrode

Zusammenfassung. Rutheniumkomplexe einiger Carborane wurden mit Hilfe zyklischer Voltammetrie, Chronoamperometrie, Chronopotentiometrie und digitaler Simulationstechniken im Zusammenhang mit Konvolutions-Dekonvolutions-Voltammetrie untersucht. Die Komplexe sind vom Typ X-RuC$_2$B$_8$H$_{10}$ (X = Hexamethylbenzol oder Paracumol). Alle relevanten elektrochemischen und chemischen Parameter wurden abgeleitet; ein Reaktionsmechanismus wird vorgeschlagen.

Introduction

The electrochemical behaviour of simple boron compounds, boranes, metalloboranes, carboranes, and metallocarboranes has been reviewed by *Morris et al.* [1]. They have analyzed the electrochemical data in view of the formal structural relationship of borane clusters with the number of electron pairs available for bonding.

A series of *closo*-metalloboranes have been examined by cyclic voltammetry. The reduction waves are reversible one-electron processes; the oxidations are irreversible for the nickel compounds. By analogy with Ni^{4+} carborane compounds, the first reduction wave for the *closo*-nickelcaboranes has been assigned to the Ni^{4+}/Ni^{3+} couple. Similarly, a quasi-reversible reduction wave in
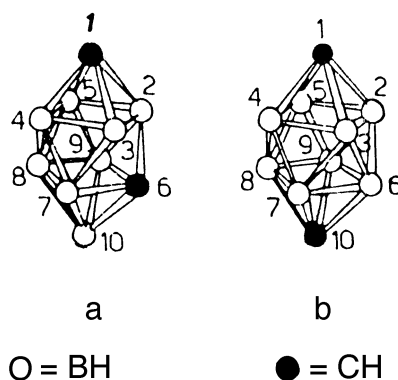
---

[*] Corresponding author

Fig. 1. Structures of *closo*-carboranes 1,6-$C_2B_8H_{10}$ (a) and 1,10-$C_2B_8H_{10}$ (b)

the Co–Ni bimetallic compounds has been assigned to the formal Co^{4+}/Co^{3+} couple [2]. Much electrochemical work has been done on mercurated carboranes [3–7]. These compounds show one polarographic reduction wave, its half-wave potential being close to the values obtained for the respective unsubstituted carboranes.

One of the interesting properties of carborane clusters is the ability of some of these compounds to undergo thermally induced isomerizations [8, 9]. A topic that must be covered as a possibility rather than a fact is the use of electrochemical methods for the purpose of opening the clusters or, in other ways, for controlling the gross structures of metallocarborane clusters. Some of the irreversible reductions of metallocarboranes may well be due to *closo*-to-*nido* or other structural changes that accompany the electron transfer step. In spite of their obvious importance, structural studies of redox-related pairs of clusters have not been widespread, obviously due to the difficulty of isolating and crystallizing the usually reactive ions found in the redox process.

The *closo*-carboranes exhibit closed polyhedral structures with triangulated faces (Fig. 1) [10]. The polyhedral carboranes can be formally viewed as derived from $B_nH_n^{2-}$ ions by replacement of BH^- groups with isoelectronic and isostructural CH groups.

In this work, the electrochemical bahaviour of some Ru-carborane complexes were determined, and proposed electrode processes at a glassy carbon electrode in non-aqueous medium and discussed. The following complexes have been investigated: **1**: (C_6Me_6)-*closo*-1,2,4-$RuC_2B_8H_{10}$, **2**: *pcym-closo*-1,2,4-$RuC_2B_8H_{10}$, **3**: *pcym-closo*-1,2,3-$RuC_2B_8H_{10}$.

Results and Discussion

*Electrochemical investigation of (C_6Me_6)-closo-1,2,4-RuC$_2$B$_8$H$_{10}$ (**1**)*

Cyclic voltammetry of a 5×10^{-3} *M* solution of (C_6Me_6)-*closo*-1, 2, 4-$RuC_2B_8H_{10}$ using a glassy carbon electrode reveals one oxidative (1 and 2) and one reductive wave (3 and 4) combined with two small oxidative peaks (5 and 6) within the CH_2Cl_2/0. 1 *M TBAP* solvent limit at temperatures between 233 and 294 K and at
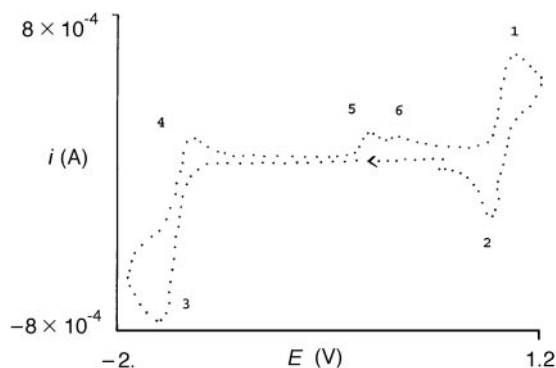
Fig. 2. Voltammogram of **1** at a glassy carbon electrode; sweep rate: 0.5 V/s, $T = 294$ K

sweep rates ranging from 0.05 to 1 V/s. Figure 2 shows a voltammogram obtained at a sweep rate of 0.5 V/s and 294 K as an example.

The electron transfer for the oxidative process of the investigated complexes was found to be quasi-reversible as indicated by the lack of overlay of the return sweep of the convoluted current upon cyclic sweeping at sweep rate of 0.2 V/s (Fig. 3). The reduction potential (E^0) was determined from the mean positions of the current peaks (Table 1). The standard heterogeneous rate constant (k_s) was extracted from the voltammograms *via* peak separation using a table of ΔE_p values *vs.* rate constants [11].

In cases of straight forward electron transfer or subsequent chemical reactions, the I_1 convolution which is defined in Refs. [12–16] as

$$I_1 = \frac{1}{\sqrt{\pi}} \int_0^t \frac{i(u)}{\sqrt{t - u}} \, du$$

allows to determine the diffusion coefficient of the bulk species to be determined from the Eq. (1) [12] where I_{lim} is the limiting value achieved for I_1 when the potential is driven to a sufficiently extreme value past the wave; the other terms have their usual significance. The values of the diffusion coefficient D corresponding to the oxidation step was calculated and is listed in Table 1.
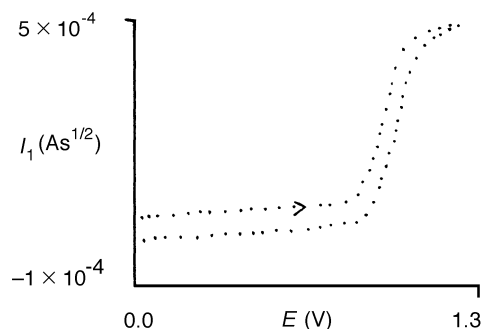
$$I_{lim} = nFAD^{1/2}C_{bulk} \tag{1}$$

Fig. 3. Convoluted current of the oxidative wave of **1** at a sweep rate of 0.2 V/s ($T = 294$ K)

Table 1. Electrochemical parameters of compounds **1–3**

| parameters | 1 | | | 2 | | | 3 | | |
	CV	CA	CP	CV	CA	CP	CV	CA	CP
$k_s \times 10^5$ (m/s)	4.10[a]	4.12[a]		2.5[a]	2.48[a]		4.1[a]	3.8[a]	
	3.44[b]			6.41[b]					
$E_{1/2}$ (V)	0.893[a]			1.04[a]			1.35[a]		
	−1.691[b]			−1.48[b]			−1.64[b]		
$D \times 10^9$ (m²/s)	4.43[a]		4.25[a]	4.20[a]		4.31[a]	3.74[a]		3.87[a]
	4.93[b]		4.71[b]	4.44[b]		4.20[b]	3.8[b]		3.9[b]
α	0.44[a]	0.42[a]		0.45[a]	0.44[a]		0.47[a]	0.45[a]	
$\Delta H^{\ddagger}$ (kJ/mol)	6.49[a]			5.38[a]			14.39[a]		
(298 K)	5.44[b]			4.71[b]			−26.88[b]		
	4.95[c]								
$\Delta S^{\ddagger}$ (J.K$^{-1}\cdot$mol^{-1})	−64.5[a]			−69.7[a]			−26.88[a]		
(298 K)	−71.9[b]			−64.04[b]					
	−36.9[c]								
$\Delta G^{\ddagger}$ (kJ/mol)	25.72[a]			26.15[a]			22.40[a]		
	26.89[b]			23.78[b]					
	15.38[c]								
k_c (s^{-1})	0.45								

CV: cyclic voltammetry, CA: chronoamperometry, CP: chronopotentiometry; [a] values of the oxidation process; [b] values of the reduction process; [c] values obtained from the plot of $\ln(k_c/T)$ *vs* $1/T$ for the reduction process

A direct test of the parameters was made by superposition of simulated voltammograms and measured data using the average experimentally determined values of the rate constant cited in Table 1 for a symmetry coefficient α of 0.44 ± 0.02. The results given in Fig. 4 employ the values for the oxidation process of compound **1** as an example and demonstrate well the agreement between experimental and simulated data. The symmetry coefficient of the oxidative wave
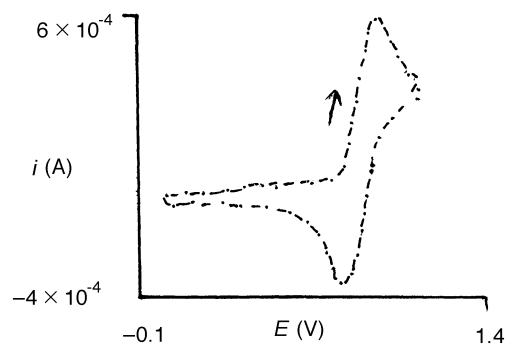

Fig. 4. Voltammograms of the oxidative wave of **1**; - - -: experimental, · · · ·: theoretical; sweep rate: 0.2 V/s, $T = 294$ K
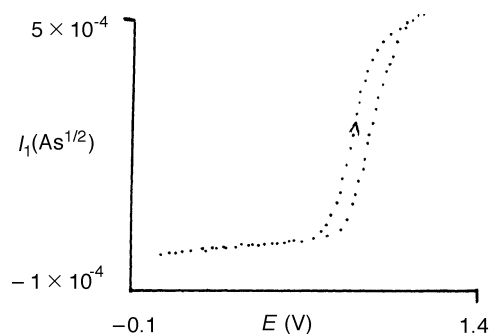
Fig. 5. Convoluted current of the oxidative wave of **1**; sweep rate: 0.5 V/s, $T = 294$ K

was evaluated directly from a chronoamperometric experiment and is in the range of 0.42 ± 0.02.

The I_1 convolution of the oxidative wave of **1** at a sweep rate of 0.5 V/s is illustrated in Fig. 5 for higher sweep rates which showed a distinct separation between the forward and reverse scan but attained a limit value past the wave and returned almost to zero at potentials before the wave. This clearly indicated the sluggishness of electron transfer and also the absence of chemical reaction or convection effects on this time scale [12]. The I_1 convolution at lower sweep rates, however, did not return to zero, indicating some observable chemical reaction occurring on the longer time scale. This behaviour can be seen in Fig. 3 and possibly arises from a depletion of the concentration of the oxidized species by a slow reaction with traces of water in CH_2Cl2 [16] and/or the presence of a decomposition process following the moderately fast electron transfer.

For both heterogeneous and homogeneous electron transfer reactions, Eq. (2) can be used for calculation of the rate constant k_s [17].

$$\ln(k_s/T) = \ln(k/h) - \frac{\Delta H^{\neq}}{RT} + \frac{\Delta S^{\neq}}{R} \tag{2}$$

From a plot of $\ln(k_s/T)$ *vs.* $1/T$, $\Delta H^{\neq}$ and $\Delta S^{\neq}$ can be extracted *via* slope and intercept, thus providing $\Delta G^{\neq}$. Values of $\Delta H^{\neq}$, $\Delta S^{\neq}$, and $\Delta G^{\neq}$ of the investigated complex are given in Table 1.

In the chronoamperometry experiment, current-time curves were recorded and subsequently treated by the Condecon software package. The rate constant k_f was calculated from Eq. (3) [18] where $u = nFAC_{bulk}k_f$ and $\beta = k_f(D)^{1/2}$. Therefore, measurements of both the intercept at $I_1 = 0$ and the slope of the linear relationship between i and I_1 give k_f.

$$i(t) = -\beta I_1 + u \tag{3}$$

An important aspect concerning the understanding of electrochemical kinetics is the fundamental relationship between the rate of the electron transfer and the potential of the electrode. This is discussed here in terms of the *Butler-Volmer* treatment which can be expressed in the form of Eq. (4) [19].

$$\ln k_f = -\frac{\alpha nF}{RT}(E_f - E_{1/2}) + \ln k_s \tag{4}$$

The linear relationship of Eq. (4) yields α from the slope and the standard heterogeneous rate constant k_s at the point at which E_f equals $E_{1/2'}$ which was found to be in agreement with the data obtained from cyclic voltammetry.

The chronopotentiometric experiment performed for the oxidation process displayed only one oxidation transition time in agreement with the single oxidative voltammetric current peak. The chronopotentiometric transition time was analyzed *via* Eq. (5) [19] where i_c is the polarization current, t_s is the transition time of the investigated compound, and the other symbols have their usual definition. It was found that the values obtained from the chronopotentiometric experiment for the diffusion coefficient were in good agreement with the results obtained from the convoluted current of cyclic voltammetry (Table 1).

$$I_{lim} = 2i_c(t_s/\pi)^{1/2} = (nFAD^{1/2}C_{bulk}) \tag{5}$$

Switching the potential to negative direction, the results given in Fig. 2 indicate that the reduction process is chemically irreversible. This was confirmed by the large difference between the return and the initial value of the I_1 convolution of the current upon cyclic sweeping. The plateau height of the I_1 convolution yielded a diffusion coefficient according to Eq. (1) which compared well with the value obtained *via* the oxidation process. With the oxidative process, a slight resistance to electron transfer was noted by the separation of the forward and reverse scans of the I_1 convolution. The rate of electron transfer ($k_s = 3.44 \pm 0.2 \times 10^{-5}$ m/s at 294 K) was determined from a working curve of CV peak separation [11]. The reduction potential E^0 of the complex was determined from the mean potential of the positions of the current peaks of the voltammogram (Table 1).

The kinetic convolution data of the reductive peak of **1** expressed according to Ref. [12] as

$$I_2 = \frac{1}{\sqrt{\pi}} \int_0^t \frac{i(u) \cdot \exp(-k_c(t-u))}{\sqrt{t-u}} \, du$$

are presented in Fig. 6 as calculated from the appropriate value of the chemical rate constant obtained by inserting trial values of the homogeneous rate constant (k_c) into the convolution calculation until I_2 returned to zero immediately after the
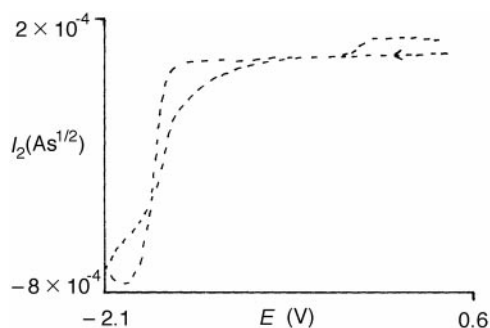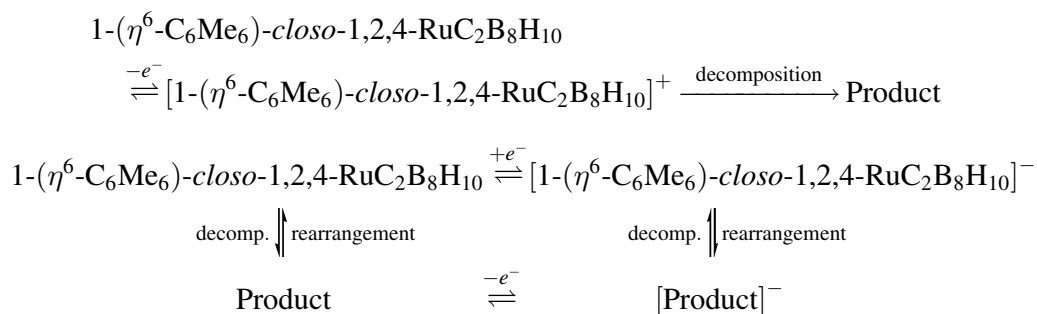

Fig. 6. Kinetic convoluted current (I_2) of the reductive process of **1** at a sweep rate of 0.2 V/s ($T = 294$ K)

wave. This is merely a reflection of the absence of the reductive species of complex under investigation at the electrode at potentials before the wave when the bulk concentration of this species is zero. On the reverse sweep where the reduced complex is oxidized I_2 reached positive values. This indicates that the square scheme might encompass the observed behaviour [20]. The true value of k_c was found to be 0.45/s at 294 K. The activation parameters for the chemical reaction following the charge transfer of the complex were extracted from the dependence of the homogeneous rate constant k_c on the temperature [12]. The values of $\Delta G^{\neq}$ are summarized in Table 1.

The dependence of the heterogeneous rate constant k_s from the temperature for the reductive process led to the evaluation of $\Delta H^{\neq}$ and $\Delta S^{\neq}$ and, consequently, $\Delta G^{\neq}$ from the analysis of the plots of $\ln(k_s/T)$ against $1/T$ (Table 1). From the electrochemical behaviour, the reduction process of the complex can be viewed as proceeding *via* EC (electron transfer followed by a chemical process), whereas the decomposition/isomerization processes associated with the reduction process yields a further product to be oxidized.

The diffusion coefficient of the bulk species evaluated from cyclic voltammetry was supported by chronopotentiometric measurements and amounts to $4.71 \pm 0.2 \times 10^{-9}$ m^2/s which confirms the value calculated from convolutive cyclic voltammetry ($4.93 \pm 0.2 \times 10^{-9}$ m^2/s) and from chronopotentiometry in the oxidative direction.

From the above electrochemical behaviour, the oxidative and reductive electrode processes can be summarized as given below.

$$1\text{-}(\eta^6\text{-}C_6Me_6)\text{-}closo\text{-}1,2,4\text{-}RuC_2B_8H_{10}$$

$$\overset{-e^-}{\rightleftharpoons} [1\text{-}(\eta^6\text{-}C_6Me_6)\text{-}closo\text{-}1,2,4\text{-}RuC_2B_8H_{10}]^+ \xrightarrow{\text{decomposition}} \text{Product}$$

$$1\text{-}(\eta^6\text{-}C_6Me_6)\text{-}closo\text{-}1,2,4\text{-}RuC_2B_8H_{10} \overset{+e^-}{\rightleftharpoons} [1\text{-}(\eta^6\text{-}C_6Me_6)\text{-}closo\text{-}1,2,4\text{-}RuC_2B_8H_{10}]^-$$

decomp. $\|$ rearrangement   decomp. $\|$ rearrangement

Product $\overset{-e^-}{\rightleftharpoons}$ $[\text{Product}]^-$

*Electrochemical studies of pcym-closo-1,2,4-Ru-C$_2$B$_8$H$_{10}$ (**2**)*

The cyclic voltammograms of a 5×10^{-3} *M* solution of **2** at a GCE in CH$_2$Cl$_2$/0.1 *M* TBAP at sweep rates ranging from 0.05–1 V/s revealed a single oxidative wave (1 and 2) and a single reductive wave (3 and 4) with a small associated wave (5) (Fig. 7).

For the oxidation process there was some evidence of a following chemical reaction at the lowest sweep rates used. Fig. 8A shows this *via* an example of a I_1 convolution of the oxidative wave at a sweep rate of 0.1 V/s. The slight deviation between the experimental and simulated curves in the reverse direction might be due to slow conversion/decomposition of **2** and was evident only at the longer time scale [20]. The failure of I_1 to return to near zero at potentials before the wave at lower sweep rates may be taken as a proof.
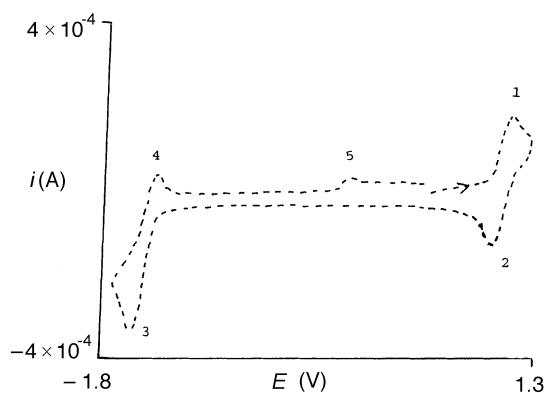
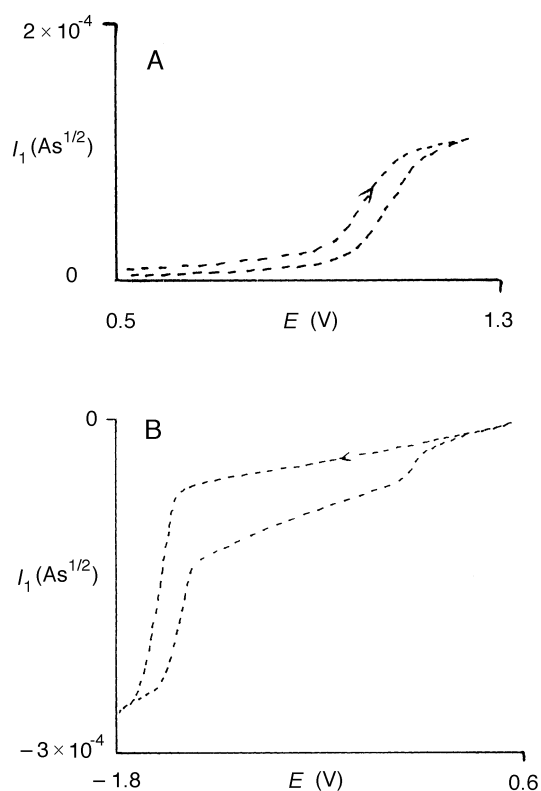**Fig. 7.** Voltammogram of **2** at a sweep rate of 0.5 V/s ($T = 294$ K)

Fig. 8. A: Convoluted current of the oxidative process of **2** at a sweep rate of 0.1 V/s ($T = 294$ K);
B: convoluted current of the reductive process of **2** at a sweep rate of 1 V/s ($T = 294$ K)

The reduction process was found to behave according to an EC scheme. The reduction wave (3+4) was definitely associated with a small oxidative peak (5) located at a peak potential around -0.046 V, since the latter is not present when the cathodic potential scan is terminated before the reductive peak (3+4). There was no observable cathodic peak coupled directly to the small oxidative peak 5 at any scan rate used confirming the EC nature of the peak 5 with a fast chemical reaction.

The behaviour of I_1 upon cycling indicated that each of the chemical reactions was most probably an isomerization since I_1 returned to zero when both waves were encompassed [12] (Fig. 8B).

The deconvolution of the current (dI_1/dt) revealed the asymmetry of the forward and reverse sweep behaviour, further confirming the EC nature of the reduction process.

Electrochemistry of pcym-closo-1,2,3-RuC$_2$B$_8$H$_{10}$ (3)

Cyclic voltammetry of **3** was performed with a 5×10^{-3} M solution in CH$_2$Cl$_2$/ 0.1 M TBAP at temperatures ranging from 233 to 294 K. A variety of sweep rates ranging from 0.05 to 1 V/s was used. Scanning the potential in positive direction revealed one oxidative wave with peaks (1) and (2), whereas upon scanning negatively a reductive wave with peaks (3) and (4) and an associated small anodic peak (5) was observed (Fig. 9).

Switching off the potential at the end of the associated oxidative peak 5 revealed the absence of its reduction peak, indicating that the chemical process following the associated oxidative electron transfer is fast.
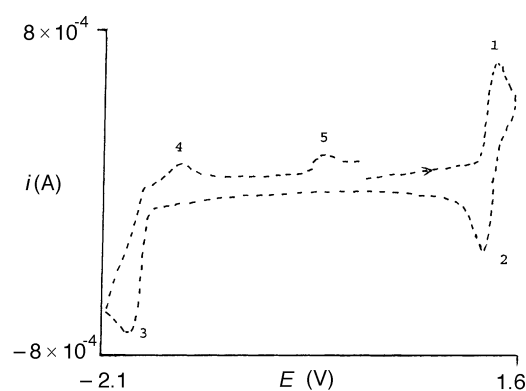

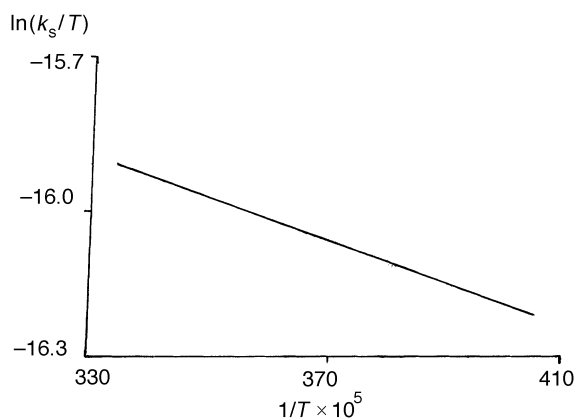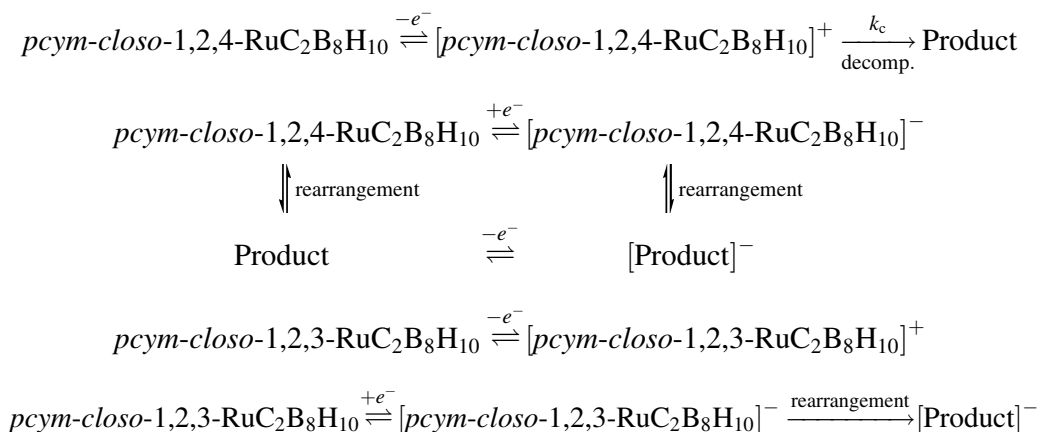**Fig. 9.** Voltammogram of **3** at a sweep rate of 0.5 V/s ($T = 294$ K)

Fig. 10. Plot of ln(k_s/T) *vs.* 1/T for the oxidation process of **3**

The deconvolution data of the reduction process revealed the inequality of peaks 3 and 4, thus confirming the EC nature of the initial reductive process. The I_1 convolution of the oxidative process returned to the initial point, indicating a simple electron transfer for this step.

The values of electrochemical and thermodynamic parameters of the two complexes **2** and **3** were calculated in the same manner as for **1** and are summarized in Table 1. An example of a plot of $\ln(k_s/T)$ against $1/T$ for the oxidation process of compound **3** is shown in Fig. 10.

Based on the electrochemical behaviour of the investigated complexes **2** and **3** the electrode mechanisms can be imagined as given below.

$$pcym\text{-}closo\text{-}1,2,4\text{-}RuC_2B_8H_{10} \overset{-e^-}{\rightleftharpoons} [pcym\text{-}closo\text{-}1,2,4\text{-}RuC_2B_8H_{10}]^+ \xrightarrow[\text{decomp.}]{k_c} \text{Product}$$

$$pcym\text{-}closo\text{-}1,2,4\text{-}RuC_2B_8H_{10} \overset{+e^-}{\rightleftharpoons} [pcym\text{-}closo\text{-}1,2,4\text{-}RuC_2B_8H_{10}]^-$$

$\updownarrow$ rearrangement $\qquad\qquad\qquad$ $\updownarrow$ rearrangement

$$\text{Product} \qquad \overset{-e^-}{\rightleftharpoons} \qquad [\text{Product}]^-$$

$$pcym\text{-}closo\text{-}1,2,3\text{-}RuC_2B_8H_{10} \overset{-e^-}{\rightleftharpoons} [pcym\text{-}closo\text{-}1,2,3\text{-}RuC_2B_8H_{10}]^+$$

$$pcym\text{-}closo\text{-}1,2,3\text{-}RuC_2B_8H_{10} \overset{+e^-}{\rightleftharpoons} [pcym\text{-}closo\text{-}1,2,3\text{-}RuC_2B_8H_{10}]^- \xrightarrow{\text{rearrangement}} [\text{Product}]^-$$

Experimental

Convolutive cyclic voltammetry, chronoamperometry, and chronopotentiometry were performed using a PAR Model 363 potentiostat and PAR Model 175 Universal Programmer (from EG & G). The system allowed the use of any scan rate up to 100 V/s for the cyclic voltammetric experiment.

Digital simulation of data for the cyclic voltammetric experiments was carried out on the Amstrad computer PC 1640. The digital simulation was used for evaluation of the accurate values of electrochemical parameters. The direct method for the determination of the parameters consisted in the superposition of the simulated voltammogram on the experimental data using the average experimentally determined values.

The electrochemical cell was equipped with a glassy carbon electrode (Metrohm Ltd) as a working electrode. Reference electrodes were made from silver wire in contact with saturated lithium chloride in dichloromethan/*TBAP* (tetrabutylammonium perchlorate) systems. The counter electrode consisted of a platinum sheet. All working solutions were degassed thoroughly with oxygen-free nitrogen, and an atmosphere of nitrogen was maintained above the solution throughout the course of an experiment.

CH_2Cl_2 was of AR grade, *TBAP* of polarographic grade; both were used as supplied (Fluka AG). Nitrogen was oxygen-free grade (BOC Limited). The metallocarborane complexes under investigation were prepared by and obtained from Dr. *J. Kennedy* [21], Leeds University. The experiments were run at temperatures ranging from 295 to 235 K.

References

[1] Morris JH, Gysling HJ, Reed D (1985) Chem Rev **85**: 51
[2] Leyden RN, Sullivan BP, Baker RT, Hawthorne MF (1978) J Am Soc **100**: 3758

 [3] Zakharkin LI, Bregadze UI, Okhlobystin O Yu (1966) J Organomet **228**: 228
 [4] Zakharkin LI, Podvisotskaya LS (1967) J Organomet Chem **7**: 385
 [5] Butin KP, Kashin AN, Beletskaya IP, German LS, Polishchuk VR (1970) J Organomet Chem **25**: 11
 [6] Zakharkin LI, Kalinin VN, Podvisotskaya LS (1968) Izv Akad Nauk Ser Khim 679
 [7] Kampel VT, Butin KP, Bergadze VI, Godovikov N (1978) Izv Nauk SSSR Ser Khim 1508
 [8] Paxson TE, Kaloustian MK, Tom GM, Wiersema RJ, Hawthorne MF (1971) J Am Chem Soc **94**: 4882
 [9] Warren LF, Hawthorne MF (1970) J Am Chem Soc **92**: 1157
[10] Grimes RN (1982) Metal Interaction With Boron Clusters. New York, p 174
[11] Nicholson RS (1965) Anal Chem **37**: 1351
[12] Blagg A, Carr SW, Cooper GR, Dobson ID, Gill JB, Goodal DC, Shaw BL, Taylor N, Boddington T (1985) J Chem Soc Dalton Trans 1213
[13] Grenness M, Oldham KB (1972) Anal Chem **44**: 1121
[14] Oldham KB, Spanier J (1970) J Electroanal Chem Interfacial Electrochem **26**: 331
[15] Dobson ID, Taylor N, Tipping LRH (1986) In: Electrochemistry Sensor and Analysis. Elsevier, Amsterdam, pp 61–77
[16] Leddy J, Bard AJ (1985) J Electroanal Chem **189**: 203
[17] Marcus RA (1968) Electrochimica Acta **13**: 995
[18] Oldham KB (1983) Anal Chem **9**: 145
[19] Warner TE (1988) PhD Thesis, University of Leeds
[20] Blackwell NK (1988) PhD Thesis, University of Leeds
[21] Kennedy J, University of Leeds (private communication)